Arch. Metall. Mater. **71** (2026), 3, 813-824

DOI: https://doi.org/10.24425/amm.2026.1972

MATEUSZ MORAWIEC[1#], JAROSŁAW OPARA[2*#], ADAM SKOWRONEK[1],
MOHAMMED ELMELIGY[3], ADAM GRAJCAR[3*]

EFFECT OF INTERCRITICAL ANNEALING ON MARTENSITE START TEMPERATURE AND LOW-TEMPERATURE BAINITIC TRANSFORMATION IN Al-ALLOYED 3Mn MULTIPHASE STEEL

The primary objective of this study was to determine how intercritical annealing affects the martensite start temperature and subsequent low-temperature bainitic transformation in a 0.17C-3.1Mn-1.6Al-0.2Si-0.2Mo-0.04Nb medium-manganese multiphase steel. A two-step heat treatment was designed, consisting of intercritical annealing in the range of 780-870°C, followed by isothermal holding at 200-300°C. The transformation behaviour was analysed using dilatometric measurements, thermodynamic calculations and scanning electron microscopy. Increasing the intercritical annealing temperature from 780°C to 870°C increased the martensite start temperature from approximately 170°C to 305°C. Lower annealing temperatures promoted stronger carbon and manganese enrichment of austenite, but reduced the amount of austenite available for bainitic transformation. The dilatometric response during isothermal holding increased with higher annealing and holding temperatures. Martensitic transformation during final cooling was detected after intercritical annealing at 780°C followed by isothermal holding at 200°C, and after intercritical annealing at 800°C followed by isothermal holding at 220°C. The most favourable response in terms of forming refined bainitic products was obtained after intercritical annealing at 860 or 870°C followed by isothermal holding at 300°C, where measurable bainitic transformation was combined with no clear martensitic signal during final cooling. The proposed route is therefore promising for further optimisation, although high-resolution characterisation is still required to confirm nanobainitic morphology and quantify phase fractions.

Keywords: Medium-Mn steel; intercritical annealing; martensite start temperature; bainitic transformation; austenite stability; dilatometry; thermodynamic calculations

1. Introduction

Medium-Mn steels constitute an important group of third-generation advanced high-strength steels because they offer a favourable balance between alloying cost, strength, and ductility [1,2]. Their mechanical properties are strongly influenced by the amount, morphology, and stability of austenite retained or formed during intercritical treatment [3-7]. In such steels, austenite stability is controlled mainly by chemical enrichment in C and Mn, the austenite fraction, grain or lath size, and the thermal or mechanical path applied after annealing [3,8-10].

Intercritical annealing (IA) is widely used to control the phase constitution of multiphase and medium-Mn steels [8,11-16]. During intercritical annealing in the ferrite-austenite region, carbon and manganese partition from ferrite to austenite, leading to chemical enrichment and enhanced thermal stability of the austenitic phase [8,9,12,14,16]. This enrichment decreases the martensite start (M_s) temperature and improve the thermal stability of austenite during final cooling [10,17-19]. At the same time, the intercritical annealing temperature determines the amount of austenite available for subsequent transformations [11,12,15,16]. Therefore, a lower IA temperature can produce chemically more stable austenite but in a smaller amount, whereas a higher IA temperature can increase the austenite fraction while reducing its chemical stabilization.

The design of low-temperature bainitic transformation in medium-Mn steels is challenging because the same alloying elements that stabilize austenite may also retard the bainitic transformation [17,18,20-23]. Carbon lowers the M_s temperature and stabilizes austenite, but can also retard the bainitic transformation and shift transformation kinetics to longer times [18,24,25]. Manganese similarly stabilizes austenite and can

[1] SILESIAN UNIVERSITY OF TECHNOLOGY, FACULTY OF MECHANICAL ENGINEERING, MATERIALS RESEARCH LABORATORY, 18A KONARSKIEGO STR., 44-100 GLIWICE, POLAND
[2] ŁUKASIEWICZ RESEARCH NETWORK – UPPER SILESIAN INSTITUTE OF TECHNOLOGY, 12-14 K. MIARKI STR., 44-100 GLIWICE, POLAND
[3] SILESIAN UNIVERSITY OF TECHNOLOGY, FACULTY OF MECHANICAL ENGINEERING, DEPARTMENT OF ENGINEERING MATERIALS AND BIOMATERIALS, 18A KONARSKIEGO STR., 44-100 GLIWICE, POLAND

[#] These two authors contributed equally to this work

* Corresponding authors: adam.grajcar@polsl.pl; jaroslaw.opara@git.lukasiewicz.gov.pl

reduce the chemical driving force for bainitic ferrite formation [17,18,20-22]. In Al-alloyed medium-Mn steels, aluminium can increase the driving force for ferrite or bainitic ferrite formation and suppress carbide precipitation, but the resulting transformation path still depends strongly on the balance between austenite stability and transformation kinetics [16,22,23,26,27].

One possible strategy is to use intercritical annealing prior to low-temperature isothermal holding (IH). In this approach, IA is intended to adjust the amount and chemical composition of austenite so that the M_s temperature is reduced below or close to the selected IH temperature. Subsequent holding at 200-300°C may then promote low-temperature bainitic transformation in the austenitic regions that remain transformable. This strategy is related to the general concept of producing very fine bainitic morphologies at low transformation temperatures, although classical nanobainitic treatments usually require longer holding times and are most often discussed for higher-carbon steels [28-30]. It is particularly important for lean 3Mn steels, where the alloying level is lower than in many medium-Mn grades but still sufficient to strongly affect austenite stability and bainitic transformation kinetics [17-20, 22,23,26].

The present work aims to determine how the intercritical annealing temperature influences the martensite start temperature and the subsequent low-temperature bainitic transformation response in a 0.17C-3.1Mn-1.6Al-0.2Si-0.2Mo-0.04Nb steel. The study combines dilatometric analysis, SEM observations, and thermodynamic calculations. The work focuses on the design of a two-step heat-treatment route and on the interpretation of the relationship between IA temperature, austenite stability, M_s temperature, and the dilatometric response during isothermal holding.

2. Material and experimental procedure

The investigated material was a laboratory-produced medium-Mn steel with the following chemical composition, expressed in wt.%: 0.17C-3.1Mn-1.6Al-0.2Si-0.2Mo-0.04Nb. The alloy was melted, cast, hot-forged, and subsequently hot-rolled in the temperature range of 1200-900°C to a final thickness of 4.5 mm. Cylindrical specimens with a diameter of 4 mm and a length of 10 mm were machined along the rolling direction for dilatometric testing.

A two-step heat-treatment route (see Fig. 1) was designed to modify the stability of intercritical austenite and to promote low-temperature bainitic transformation during subsequent isothermal holding. The first step consisted of intercritical annealing in the temperature range of 780-870°C for 60 min. The second step consisted of cooling at 60°C/s to the selected isothermal holding temperature in the range of 200-300°C, followed by holding for up to 4 h. The investigated processing variants are listed in TABLE 1.

The IA and IH temperatures were not selected as a uniformly spaced temperature grid, but were chosen to represent different levels of austenite enrichment and different experimentally determined M_s temperatures. The IA range of 780-870°C was selected to cover conditions from a low austenite fraction with

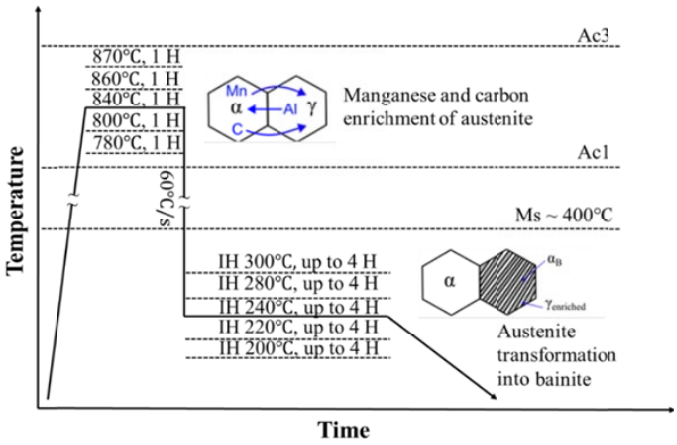

Fig. 1. Schematic representation of the two-step heat-treatment route consisting of intercritical annealing (IA) followed by low-temperature isothermal holding (IH). The scheme illustrates the intended formation of: α – ferrite, α_B – bainitic ferrite, and γ – austenite

strong C and Mn enrichment (lower temperatures) to a higher austenite fraction with lower chemical enrichment and a higher M_s temperature (higher temperatures). Therefore, the interval between 800 and 840°C was intentionally used to include a transition from strongly stabilised austenite to conditions with a markedly higher amount of austenite available for bainitic transformation. The additional IA temperature of 870°C was introduced to verify the effect of approaching the upper part of the intercritical region. The IH temperatures were selected close to or above the corresponding M_s temperatures after IA (after the IA and corresponding austenite enrichment in C and Mn the M_s temperatures decrease), in order to promote low-temperature bainitic transformation while limiting unwanted direct martensitic transformation during cooling. For this reason, the experimental matrix included selected representative IA/IH combinations rather than all intermediate temperatures, such as 820°C for IA or 260°C for IH.

TABLE 1

Heat treatment temperatures used in the experiment

IA temperature [°C]	IH temperature [°C]	Code of the variant
780	200	IA780/IH200
780	300	IA780/IH300
800	220	IA800/IH220
800	240	IA800/IH240
840	280	IA840/IH 280
860	300	IA860/IH300
870	300	IA870/IH300

The heat treatments were performed using a Bähr DIL 805 A/D dilatometer under vacuum. Helium was used for rapid cooling. Temperature was measured using an S-type thermocouple welded to the central part of each specimen. The martensite start temperature was determined from the dilatometric curves during cooling according to the general procedure of ASTM A1033-04 [31]. The relative change in length (RCL) during isothermal holding was used as a qualitative indicator of the progress of the

bainitic transformation. It should be emphasized that this dilatometric signal was not treated as a direct quantitative of bainite phase fraction. The stability of austenite after IH was assessed by analysing whether an additional martensitic transformation signal occurred during final cooling to room temperature.

After heat treatment, the specimens were sectioned perpendicular to their longitudinal axis and prepared using standard metallographic procedures. The samples were ground with SiC papers up to 2000, polished using 3 µm, 1 µm diamond pastes, and etched with 2% nital. Microstructural observations were performed by scanning electron microscopy (SEM) using secondary electron imaging at an accelerating voltage of 20 kV with Zeiss Supra 25 and JEOL microscopes. The SEM observations were used as qualitative support for identifying ferritic, martensitic, and bainite-containing regions.

Thermodynamic calculations were performed to support the interpretation of the dilatometric results. Equilibrium phase constitution and the chemical composition of austenite after intercritical annealing were calculated using JMatPro with the general steel module [32]. Additional equilibrium phase-fraction calculations and martensite start temperature calculations were performed using Thermo-Calc software, utilizing the TCFE11 and MOBFE8 databases, with the Property Calculator module [33]. The T_0 and T_0' conditions and/or the Gibbs free-energy difference between austenite and bainitic ferrite were performed using MAP_STEEL_MUCG83 programme [34]. These calculations were used to interpret thermodynamic tendencies only. They do not describe the full transformation kinetics, local chemical heterogeneity, or possible non-equilibrium partitioning during finite-time annealing.

3. Results

3.1. Effect of intercritical annealing temperature on martensite start temperature

The influence of intercritical annealing temperature on the martensite start temperature is shown in Fig. 2, and the corresponding M_s values are summarized in TABLE 2. A clear increase in M_s was observed with increasing IA temperature. After IA at 780°C, the M_s temperature was approximately as low as 170°C, whereas after IA at 870°C it increased to approximately 305°C.

This trend indicates that lower IA temperatures produce austenite with higher thermal stability during subsequent cooling, which was evidenced by SEM in Fig. 3a and b. A lot of

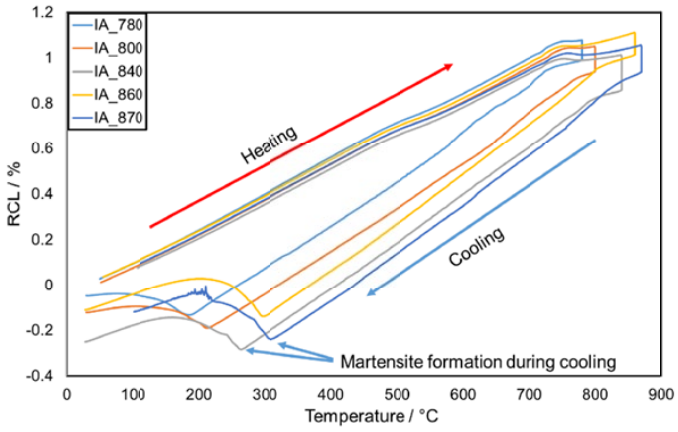

Fig. 2. Dilatometric cooling curves used to determine the effect of IA temperature on the martensite start temperature of intercritical austenite

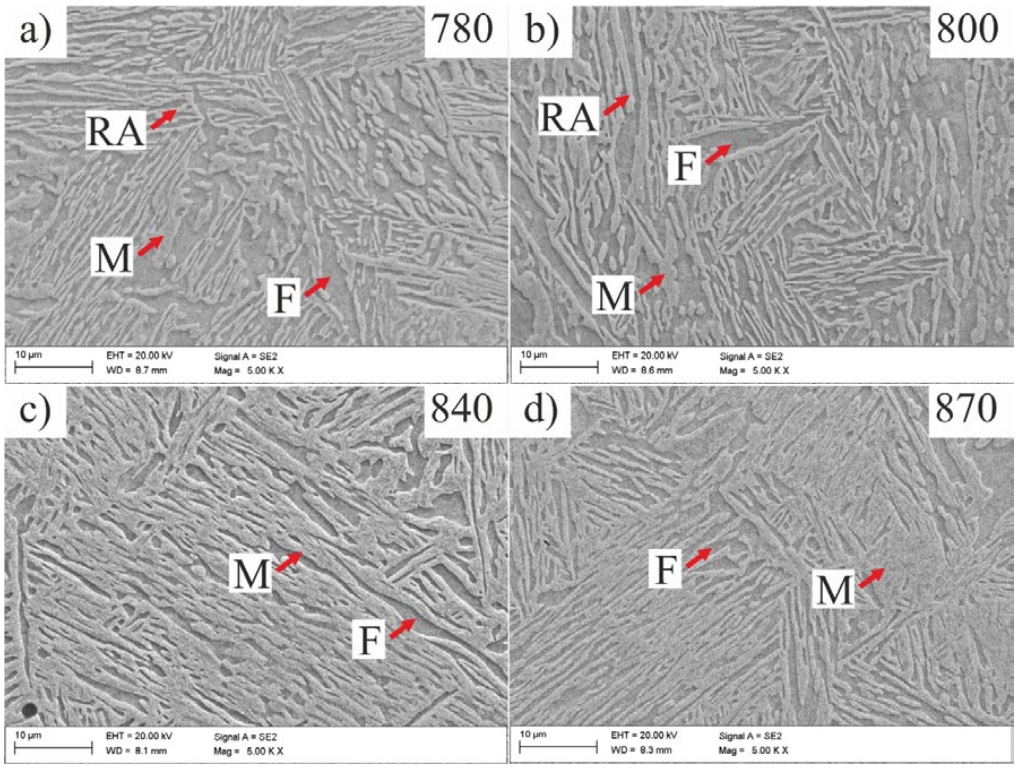

Fig. 3. SE M microstructures of the investigated steel after selected intercritical annealing treatments; F – ferrite, RA – retained austenite, M – martensite

austenite is stable up to room temperature (RA) with only large blocky austenite grains transformed to martensite (M) in a final cooling step (Fig. 2). This behaviour is consistent with the expected phase equilibrium in the intercritical region. At lower IA temperatures, the ferrite fraction is higher and the amount of austenite is lower. Consequently, carbon and manganese are distributed into a smaller volume fraction of austenite, leading to stronger chemical stabilization and a lower M_s temperature. With increasing IA temperature, the fraction of ferrite decreases and austenite increases (Fig. 3c and d), and the average enrichment of austenite in stabilizing elements decreases. As a result, austenite becomes less stable and transforms entirely to martensite at higher temperatures during cooling.

TABLE 2

Experimentally determined M_s temperatures for different IA temperatures

IA temperature / °C	780	800	840	860	870
M_s temperature / °C	170	210	260	300	305

3.2. Effect of IA temperature on the dilatometric response during isothermal holding

The dilatometric response during isothermal holding at 300°C is presented in Fig. 4 for selected IA temperatures. The curves show that the IA temperature affects both the rate and the magnitude of the transformation-related length change during IH. Samples annealed at higher IA temperatures exhibited a stronger dilatometric response, defined here as a larger RCL during isothermal holding. This indicates that a larger fraction of austenite was available for bainitic transformation.

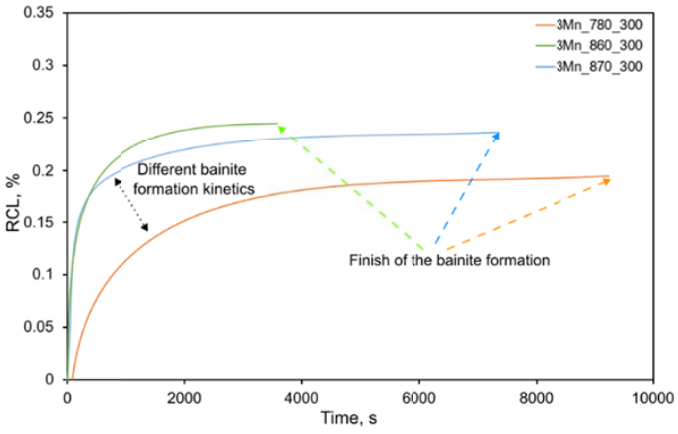

Fig. 4. Effect of IA temperature on the bainite formation kinetics during isothermal holding

The weaker dilatometric response after IA at 780°C, i.e. the smaller RCL increase during IH, can be attributed to the lower fraction of intercritical austenite formed at this temperature. Although this austenite was chemically more stable due to stronger C and Mn enrichment, its amount was limited. Therefore, only a smaller part of the microstructure could participate in the subsequent bainitic transformation. By contrast, higher IA temperatures produced a larger austenite fraction, which increased the volume of material capable of transforming during IH. However, this austenite was less enriched in carbon and manganese, because these elements were distributed over a larger austenite fraction. As a result, its thermal stability decreased and the M_s temperature increased.

The length-change signal should be interpreted as a relative indicator of transformation progress, not as a direct quantitative measurement of bainite fraction. Without independent phase-fraction measurements, such as XRD or EBSD, the amount of bainite and retained austenite cannot be quantified reliably.

3.3. Effect of isothermal holding temperature on bainitic transformation response

The effect of IH temperature on the transformation response is shown in Fig. 5. For a given IA temperature, lower IH temperatures resulted in slower transformation kinetics and a smaller length-change signal over the investigated holding time. This behaviour is expected for low-temperature bainitic transformation, where decreasing the holding temperature increases undercooling but also reduces atomic mobility and slows down transformation kinetics.

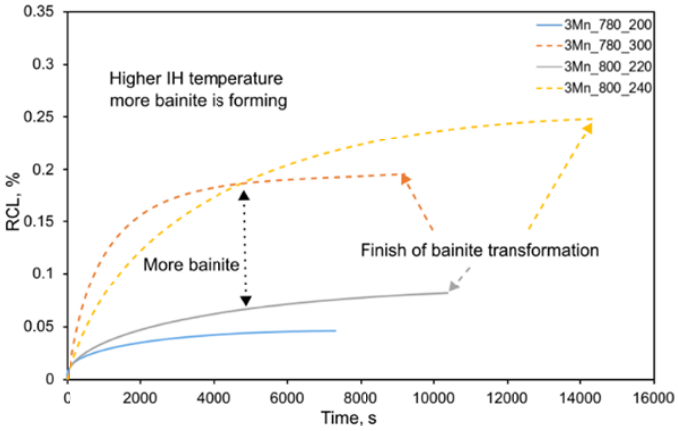

Fig. 5. Effect of isothermal holding temperature on bainite transformation kinetics

For the 780°C IA condition, holding at 200°C produced only a weak dilatometric response, whereas holding at 300°C resulted in a more pronounced length change. A similar tendency was observed for the 800°C IA condition, where increasing the IH temperature accelerated the transformation response. Therefore, the experimental results show that the IH temperature must be selected not only with respect to M_s, but also with respect to the transformation time available for bainitic reaction.

Although stronger undercooling increases the thermodynamic driving force for the bainitic transformation, the present dilatometric results indicate that at the lowest IH temperatures, especially 200-220°C, the transformation kinetics becomes in-

creasingly limited by reduced atomic mobility and carbon redistribution. Therefore, in this temperature range, diffusion-related limitations may become more important than the additional increase in the free-energy difference. However, the present experimental matrix does not allow a precise critical temperature separating these two regimes to be determined.

The results indicate that there is a processing compromise. Holding too close to a low M_s temperature may strongly slow the transformation, whereas holding at a higher temperature can accelerate the reaction but may also reduce the thermodynamic conditions favourable for forming a very fine bainitic morphology. Within the investigated processing window, the most pronounced dilatometric response was associated with higher IH temperatures, especially near 300°C. However, this should not be described as a universal optimum without additional phase-fraction and microstructural quantification.

3.4. Thermal stability of austenite during final cooling

The stability of austenite after isothermal holding was assessed from the dilatometric curves recorded during final cooling from the IH temperature to room temperature (Fig. 6). A martensitic transformation signal was detected only for the samples annealed at IA = 780°C and held at IH = 200°C, and annealed at IA = 800°C and held at IH = 220°C, hereafter referred to as the IA780/IH200 and IA800/IH220 samples, respectively. The transformation started at approximately 130°C for IA780/IH200 and at approximately 60°C for IA800/IH220, indicating that part of the austenite remaining after IH was not sufficiently stable to avoid transformation during final cooling. For the other investigated samples, no clear martensitic transformation signal was observed during cooling to room temperature. This suggests that the remaining austenite was thermally stable under the applied cooling conditions, or that any possible transformation occurred below the detection sensitivity of the dilatometric mea-surement.

The stronger martensitic signal observed for the IA780/IH200 sample indicates that the limited bainitic transformation during low-temperature holding did not provide sufficient carbon enrichment of the remaining austenite. In contrast, the absence of a martensitic signal in samples treated at higher IH temperatures suggests that bainitic transformation and carbon redistribution during IH were more effective in stabilizing the remaining austenite during final cooling.

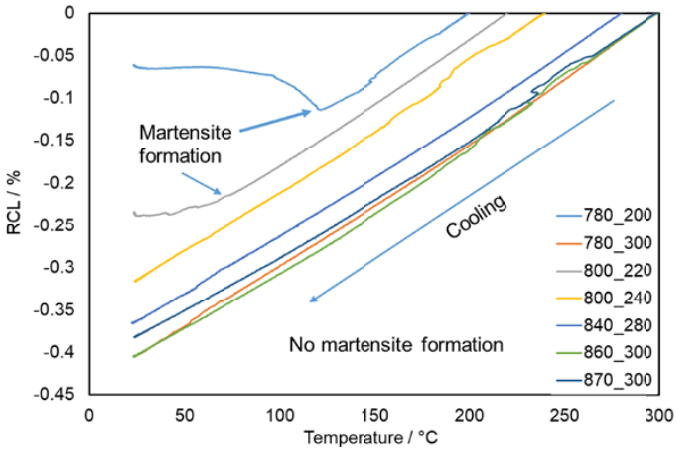

Fig. 6. Dilatometric cooling curves recorded after isothermal holding, used to assess the thermal stability of remaining austenite during cooling to room temperature

3.5. SEM observations of bainite-containing microstructures

SEM micrographs of selected heat-treatment variants are shown in Fig. 7. The microstructural analysis was based on SEM observations because this technique provides higher spatial resolution than light microscopy and is therefore more suitable for identifying refined bainitic regions, fresh martensite and ferritic areas in the investigated steel. The microstructures consist mainly of ferritic regions formed during intercritical annealing, regions of refined bainite (RB) embedded in the intercritical austenite laths, and sometimes martensitic areas formed during cooling in the less stable conditions. The fraction and morphology of these constituents depend on the IA and IH temperatures.

After IA at 780°C and IH at 200°C, the microstructure contained a substantial ferritic fraction and only limited areas that can be associated with bainitic transformation. This agrees with the weak dilatometric response observed during IH. Increasing the IA temperature increased the amount of austenite available for transformation and promoted more visible bainite-containing regions after IH, while a further increase in IA temperature above 800°C led to gradual microstructural fragmentation and an increased fraction of fine bainitic regions. Increasing the isothermal holding temperature also resulted in a substantially higher bainite fraction in the microstructure. However, the SEM evidence should be treated as qualitative. The available images do not allow reliable measurement of bainitic ferrite plate thickness and therefore do not provide direct proof of a nanobainitic morphology.

4. Discussion

The present results show that the response of the investigated 0.17C-3.1Mn-1.6Al-0.2Si-0.2Mo-0.04Nb steel to the two-step heat treatment is controlled by a balance between three coupled factors: the amount of austenite formed during intercritical annealing, its chemical enrichment in C and Mn, and the kinetics of bainitic transformation during subsequent isothermal holding. These factors do not vary independently. Lower intercritical annealing temperatures promote stronger chemical stabilization of austenite, whereas higher IA temperatures increase the amount of austenite available for further transformation. Therefore, the martensite start temperature, the dilatometric response during isothermal holding, and the stability of the remaining austenite during final cooling must be interpreted jointly rather than as separate effects.

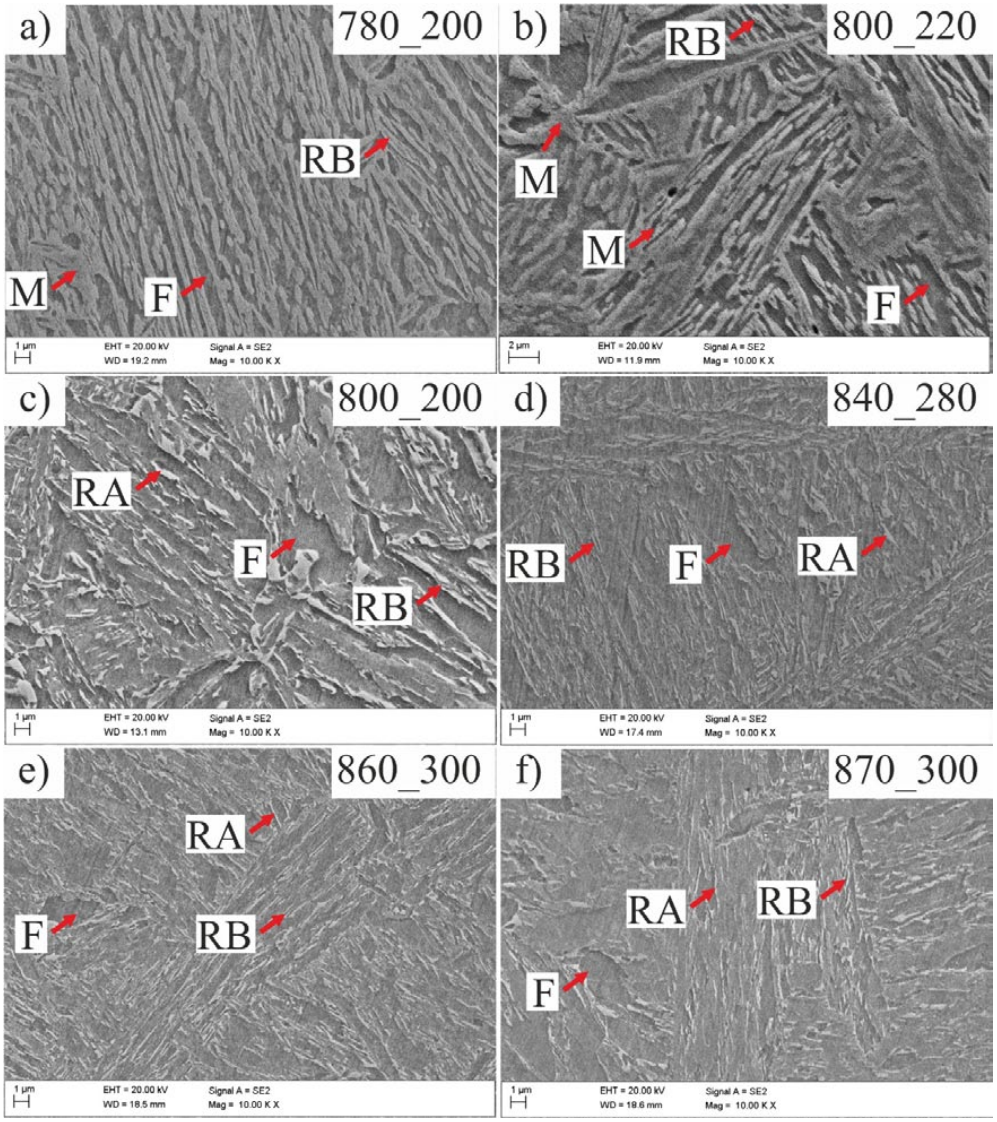

Fig. 7. SEM microstructures of the investigated steel after selected two-step heat treatments; F – ferrite, RA – retained austenite, RB – refined bainite, M – martensite

The influence of IA temperature is clearly reflected in the experimentally determined martensite start temperatures. As shown in Fig. 2 and TABLE 2, M_s increased from about 170°C after IA at 780°C to about 305°C after IA at 870°C. This trend is consistent with the expected change in phase equilibrium in the intercritical region. At lower IA temperatures, ferrite is the dominant phase and only a limited fraction of austenite is formed. Because carbon has very limited solubility in ferrite and Mn preferentially partitions to austenite, this smaller austenite fraction becomes more enriched in both elements. The JMatPro-calculated austenite compositions listed in TABLE 3 support this interpretation: the C content in austenite decreases from about 0.42 mass.% after IA at 780°C to about 0.27 mass.% after IA at 860°C, while the Mn content decreases from about 4.92 to 3.83 mass.% over the same temperature interval. Such enrichment explains the suppression of M_s after low-temperature IA.

The Thermo-Calc calculations further support this interpretation by directly linking the intercritical annealing temperature

TABLE 3

Chemical composition of the austenite after the intercritical annealing at different temperatures; values calculated by the JMatPro software

Temp. [°C]	Fe [mass.%]	Al [mass.%]	Mn [mass.%]	Mo [mass.%]	Nb [mass.%]	Si [mass.%]	C [mass.%]
860	94.15	1.36	3.83	0.18	0.0001	0.20	0.27
840	93.95	1.32	4.04	0.18	0.0001	0.21	0.30
820	93.71	1.28	4.29	0.18	0.0001	0.21	0.33
800	93.42	1.24	4.58	0.18	0.0000	0.21	0.37
780	93.07	1.20	4.92	0.18	0.0000	0.21	0.42

with the predicted phase balance and the composition-dependent martensite start temperature. These calculations complement the dilatometric results and the calculated austenite compositions listed in TABLE 3. The equilibrium phase-fraction calculation in Fig. 8 clarifies how the relative amounts of ferrite and austenite change within the intercritical temperature range, whereas the Property Calculator results in Fig. 9 illustrate the sensitivity of M_s to the carbon and manganese contents in austenite.

The equilibrium Thermo-Calc calculation shown in Fig. 8 confirms that the applied IA range is located within the ferrite-austenite intercritical region. The main phases shown in the graph (Fig. 8a) are BCC_A2, corresponding mainly to ferrite, and FCC_A1, corresponding to austenite. A secondary FCC_A1#2 phase is also predicted, but only in a negligible fraction. Minor carbide phases, namely M7C3_D101, CEMENTITE_D011, M23C6_D84 and M6C_E93, are also present in the calculation. Their low calculated fractions are shown more clearly in the enlarged view in Fig. 8b, confirming that they remain minor equilibrium constituents compared with the dominant BCC_A2 and FCC_A1 phases. Therefore, within the IA temperature range used in this study, the main effect of temperature is associated with the changing balance between ferrite and austenite. At low and intermediate temperatures, BCC_A2 remains the dominant phase. Above approximately 650–670 °C, the FCC_A1 fraction increases rapidly, while the BCC_A2 fraction gradually decreases. Both phases reach comparable fractions at around 820°C. At temperatures above approximately 940-950°C, the alloy becomes nearly fully austenitic. These results support the interpretation that the IA temperature controls both the amount of austenite available for subsequent transformation and its chemical enrichment, which in turn affects M_s and the bainitic response during IH.

The Thermo-Calc Property Calculator results presented in Fig. 9 further show that the calculated M_s temperature

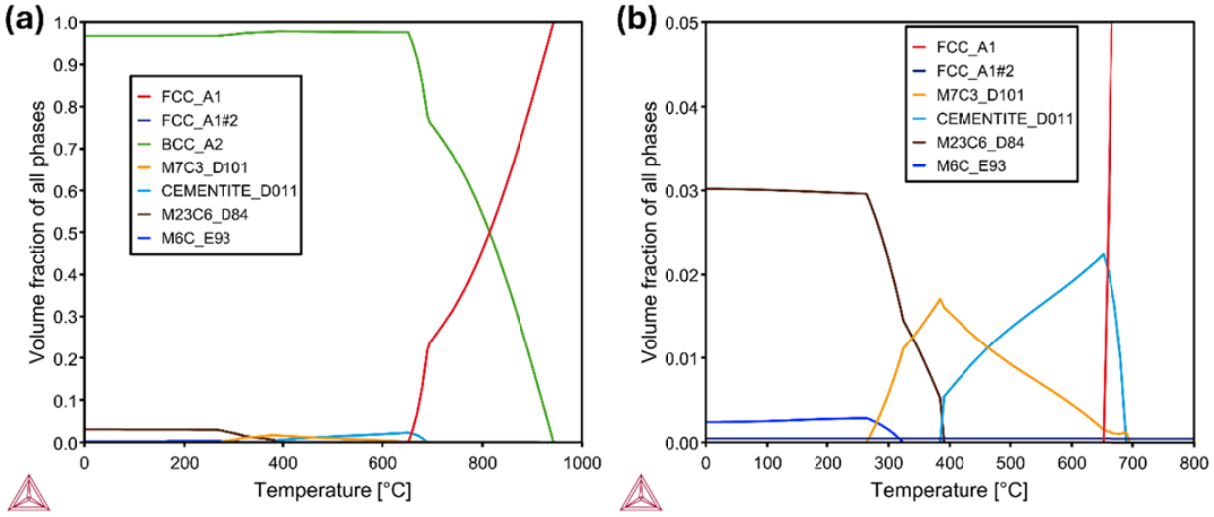

Fig. 8. Thermo-Calc equilibrium phase-fraction calculation for the investigated 0.17C-3.1Mn-1.6Al-0.2Si-0.2Mo-0.04Nb steel as a function of temperature: (a) full volume-fraction range and (b) enlarged low-volume-fraction range showing minor phases

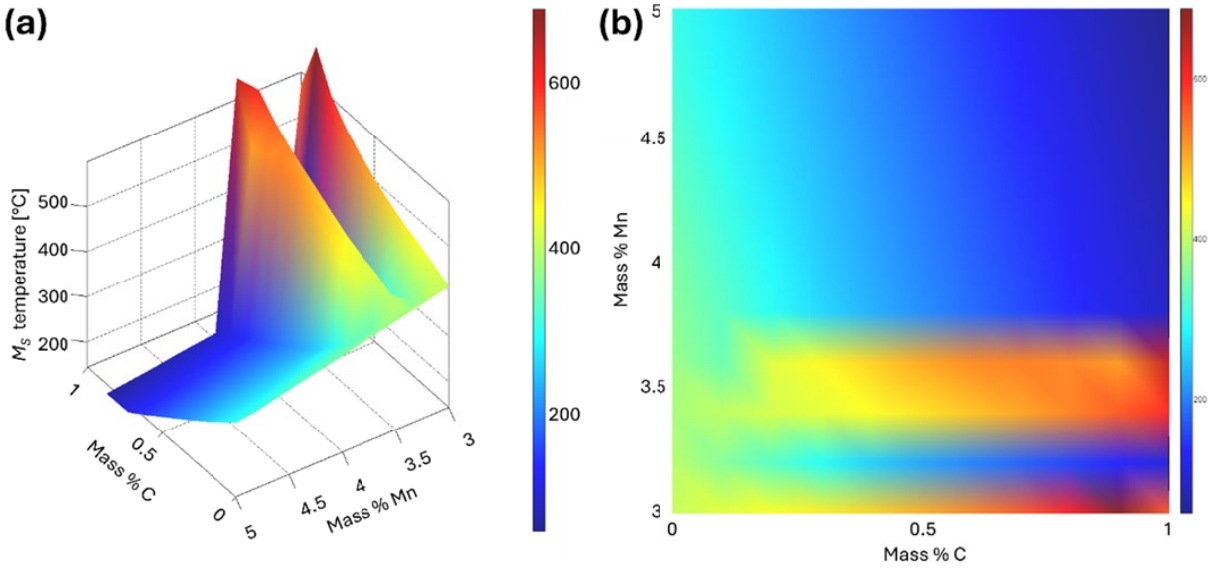

Fig. 9. Thermo-Calc Property Calculator results showing the calculated M_s temperature as a function of carbon and manganese concentration in austenite: (a) three-dimensional colour map and (b) two-dimensional colour map

is strongly controlled by the carbon and manganese contents in austenite. In these calculations, an effective austenite grain size of 30 μm was assumed as a required input parameter for the M_s calculation. This value should be treated as a representative calculation parameter rather than as an experimentally measured prior-austenite grain size. Since the initial microstructure of the investigated steel was martensitic, austenite formation during reheating is expected to be influenced by the previous lath morphology and may lead to relatively refined austenite regions. Increasing both C and Mn lowers M_s, confirming their stabilizing effect on austenite, although the influence of carbon is particularly pronounced. Manganese provides an additional decrease in M_s, especially within the composition range relevant to the present steel. Therefore, the calculated M_s values are used mainly for comparative assessment of the effect of austenite chemistry, especially C and Mn enrichment, rather than as absolute predictions fully accounting for the real austenite morphology. It should also be noted that the effective austenite grain size can influence M_s and steel properties; finer austenite grains or smaller austenite regions generally increase austenite stability, may reduce the martensite start temperature, and contribute to strengthening through microstructural refinement. These results support the interpretation that C and Mn enrichment of austenite during IA can substantially reduce its M_s temperature and thereby enable subsequent IH in the low-temperature bainitic transformation range.

This interpretation is also consistent with the literature on intercritical annealing of medium-Mn and TRIP-assisted steels. Kokosza and Pacyna reported that increasing the intercritical annealing temperature increases the amount of austenite formed in a medium-carbon TRIP steel [11]. Cai et al. showed a similar tendency in Fe-0.2C-11Mn-6Al steel, where increasing the annealing temperature from 650 to 950°C increased the austenite fraction from 42 to 50% [12]. In medium-Mn steels, Yan et al. [10], Hu and Luo [13], Lin et al. [14], Liu et al. [15], and Skowronek et al. [16] also demonstrated that the IA temperature strongly affects austenite growth, element partitioning, and the stability of retained or intercritical austenite. The present results follow the same physical tendency, although the investigated steel has a lower Mn content and contains Al, Si, Mo, and Nb additions, which modify the thermodynamic stability and transformation kinetics.

However, a lower M_s temperature alone should not be treated as evidence of a more favourable condition for bainitic transformation. The 780°C and 800°C IA variants produced chemically more stable austenite, but they also contained a smaller amount of austenite available for transformation during IH. This explains why the dilatometric response during isothermal holding may remain weak even when the austenite is strongly enriched in C and Mn. In contrast, increasing the IA temperature to 860 or 870°C reduces the chemical stability of individual austenite regions, as indicated by the higher M_s values, but it also increases the volume fraction of transformable austenite. Consequently, the transformation-related dilatometric signal during IH becomes stronger. This is particularly visible when comparing the IA780/IH300, IA860/IH300, and IA870/IH300 samples in Fig. 4. The higher IA variants produced a larger relative change in length values, which indicates a larger extent of bainitic transformation under the applied holding conditions.

In the present work, the influence of individual alloying elements was not analysed separately for all elements present in the steel. The discussion was focused mainly on carbon and manganese, because these elements showed the largest changes in austenite composition after IA and are known to strongly affect austenite stability, M_s temperature and bainitic transformation kinetics [9,20,21,24]. Carbon enrichment increases the thermal stability of austenite and strongly decreases M_s, but it can also retard bainitic transformation kinetics. Similarly, manganese stabilises austenite, decreases M_s and may reduce the chemical driving force for the $\gamma \rightarrow \alpha$ transformation, thereby slowing the bainitic reaction. This is consistent with literature data showing that higher carbon content shifts bainitic transformation to longer times, while increased manganese content decreases the driving force for bainite formation and retards transformation kinetics.

The calculated thermodynamic data further explain this behaviour. According to TABLE 3, low-temperature IA produces austenite enriched in both C and Mn. These elements increase austenite stability and reduce M_s, but they can also slow the bainitic transformation. Zhu et al. showed that higher carbon content retards bainite formation in 4140/4150 steels, shifting transformation to longer times [24]. Morawiec et al. demonstrated that increasing Mn content reduces the chemical driving force for bainitic transformation and slows the transformation kinetics in medium-Mn alloys [20]. Kim et al. analysed 0.28C-3.8Mn-1.5Si steel and showed that local Mn heterogeneity affects the driving force and, consequently, the rate of bainite formation [21]. In the present steel, the calculated driving force for the austenite-to-bainite/ferritic bainite transformation increases with increasing IA temperature, and the difference between the lowest and highest IA temperature is about 336 J/mol, according to the calculations shown in Fig. 10. Thus, the weaker bainitic response after low-temperature IA is not only a consequence of a smaller austenite fraction but also of a lower thermodynamic tendency for transformation and slower kinetics.

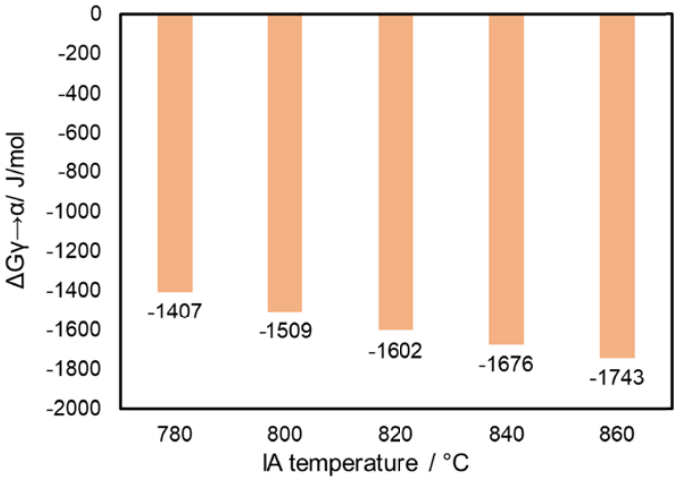

Fig. 10. Change in the Gibbs free energy between austenite and bainite calculated using MAP_STEEL_MUCG83 programme [34]

The effect of IH temperature confirms this compromise. Lower IH temperatures are generally favourable for refined bainitic morphologies because they increase undercooling below the bainite start range and promote finer bainitic ferrite plates. However, they also substantially slow the transformation rate. In the present experiments, holding at 200°C after IA at 780°C produced only a very small dilatometric response, with RCL close to 0.04%, indicating that only a limited amount of bainite-containing product formed during the applied holding time. Increasing the IH temperature to 300°C for the same IA temperature increased the transformation response, with RCL close to 0.18%. A similar effect was observed for the 800°C IA variants, where higher IH temperature resulted in a stronger transformation signal than holding close to M_s. These observations agree with the results of Pei et al., who found that decreasing the austempering temperature from 330 to 270°C increased the final bainite fraction but prolonged the transformation time from about 10000 to 28000 s in a medium-carbon bainitic steel [25]. They are also consistent with dilatometric studies of medium-Mn steels by Morawiec et al. [17], Skowronek and Kozłowska [18], Morawiec et al. [22], and Wojtacha et al. [23], where low-temperature bainitic transformation was shown to be strongly time- and composition-dependent.

The stability of austenite after IH is evidenced by the cooling curves from the holding temperature to room temperature. In the IA780/IH200 and IA800/IH220 samples fresh martensite was detected during final cooling (Fig. 6), with the martensitic signal starting at approximately 130°C and 60°C, respectively. This indicates that the bainitic transformation during IH was insufficient to enrich the remaining austenite in carbon to a level required for room-temperature stability. The effect was stronger for the IA780/IH200 sample, where the lower transformation response during IH was accompanied by a more pronounced martensitic signal during final cooling. In contrast, the variants treated at higher IH temperatures, especially IA860/IH300 and IA870/IH300, showed stronger transformation-related dilatometric responses during IH and no clear martensitic signal during final cooling. This suggests that, within the investigated range, these conditions provided a more favourable combination of a sufficient austenite fraction, adequate transformation kinetics, and improved thermal stability of the residual austenite.

The T_0 and T_0' concepts provide a useful thermodynamic framework for interpreting the incomplete character of bainitic transformation. During bainitic ferrite formation, carbon is rejected into the surrounding austenite, progressively increasing its stability. The diffusionless growth of bainitic ferrite can continue only while the free-energy condition for transformation remains favourable. When the carbon content of austenite approaches the T_0 or T_0' condition at a given temperature, further growth becomes thermodynamically restricted. In the present steel, this limitation is additionally affected by Mn enrichment of austenite. As shown schematically by the calculated T_0 relationships in Fig. 11, increasing Mn content shifts the equilibrium condition in a way that can reduce the possible extent of bainitic transformation. Therefore, the amount of bainite formed during IH depends not only on the holding temperature but also on the austenite composition inherited from IA.

This thermodynamic limitation helps explain why the chemically most stable austenite after IA is not necessarily the most favourable starting condition for bainite formation. After IA at 780°C, the austenite contains about 4.92 mass.% Mn and 0.42 mass.% C according to TABLE 3. These values lower M_s, but they also decrease the driving force and limit the transformation rate. Under the IA780/IH200 condition, the bainitic reaction was too weak to provide sufficient additional carbon enrichment of the remaining austenite, and fresh martensite appeared during final cooling. After IA at 860°C, the austenite is less enriched in C and Mn, but the larger austenite fraction and higher calculated driving force favour a stronger bainitic reaction during IH at 300°C. The resulting carbon redistribution during bainitic ferrite formation appears sufficient to stabilise the remaining austenite thermally down to room temperature, as indicated by the absence of a clear martensitic signal during final cooling.

The high magnification SEM observations support the dilatometric interpretation. The microstructures in Figs. 7 and 12

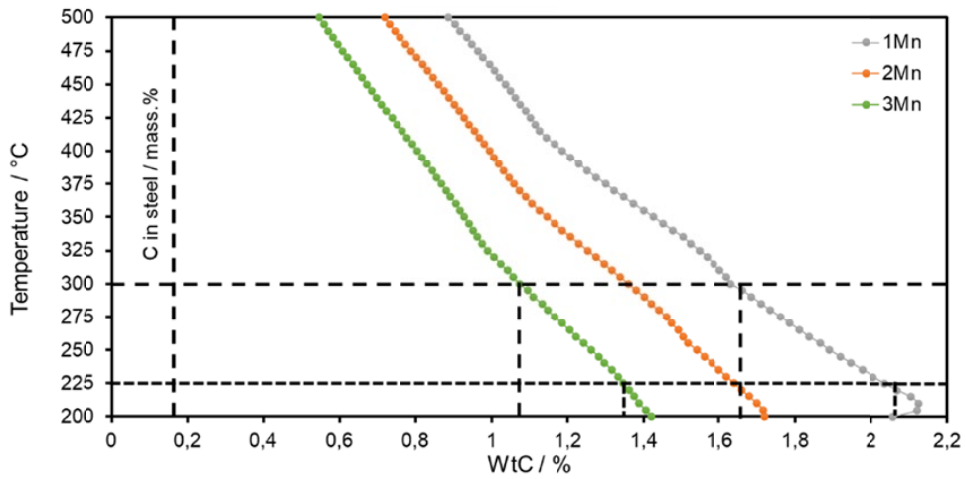

Fig. 11. The influence of the manganese content in steel on the T0 curve representing the equilibrium between austenite and bainite as a function of carbon content. Results obtained by the MAP_STEEL_MUCG83 programme [34]

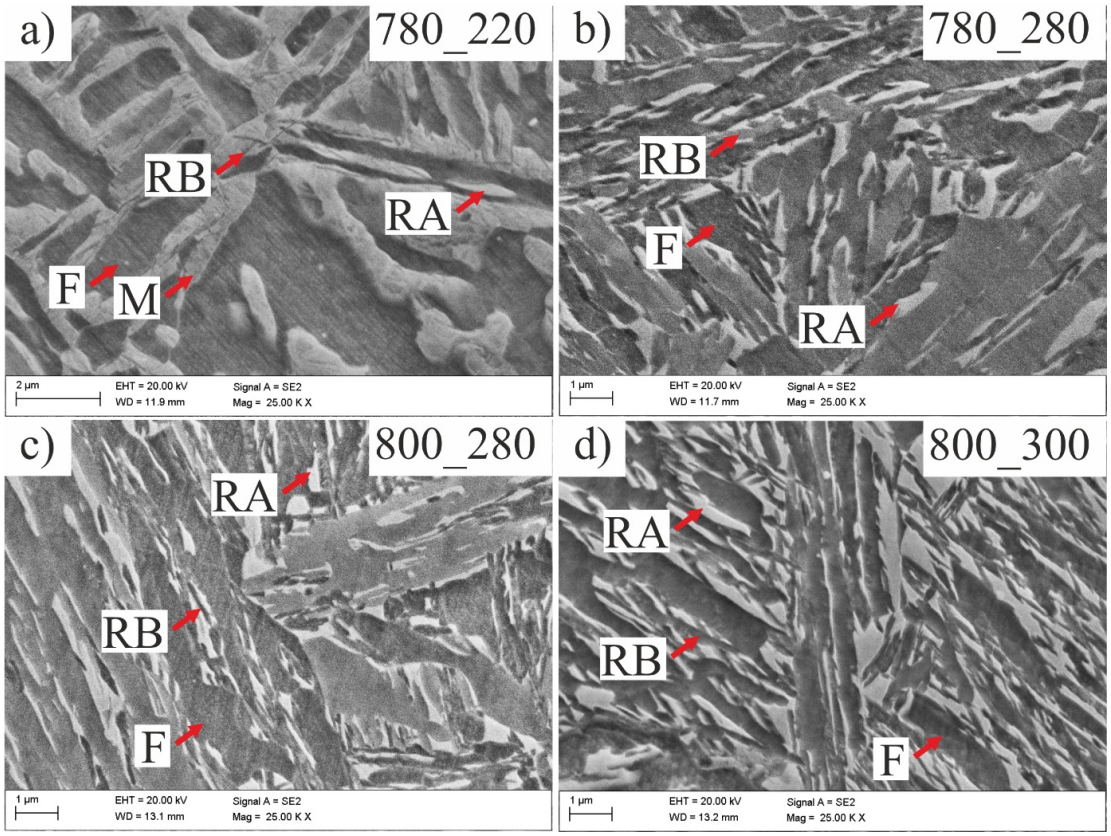

Fig. 12. High-magnification SEM microstructures of the investigated steel after selected two-step heat treatments; F – ferrite, RA – retained austenite, RB – refined bainite, M – martensite

show ferritic regions formed during IA, martensitic regions in conditions where austenite was not fully stabilised, and refined bainite-containing regions (RB) after the two-step treatment. The fraction and morphology of these regions change with IA and IH conditions in a way that is consistent with the dilatometric curves: the IA780/IH200 and IA800/IH220 samples showed only limited refined bainitic regions and evidence of fresh martensite (M), whereas the IA860/IH300 and IA870/IH300 showed a more pronounced refined bainite (RB) morphology.

Overall, the results indicate that the most favourable response within the investigated experimental range is obtained when the heat treatment combines a sufficiently high amount of transformable austenite with an IH temperature high enough to allow measurable bainitic transformation during the applied holding time. Among the tested variants, the IA860/IH300 and IA870/IH300 samples provided the strongest transformation-related dilatometric responses and satisfactory thermal stability during final cooling. These variants should therefore be described as the most favourable among the investigated conditions, while the broader optimisation of IA and IH parameters remains a subject for further study.

The present study supports the concept of using intercritical annealing to reduce the effective M_s temperature of austenite and enable subsequent low-temperature bainitic transformation in a lean Al-alloyed medium-Mn steel. At the same time, it shows that the process is governed by a trade-off between austenite chemical stability and the amount of austenite available for bainitic transformation. The approach is promising for further development of refined bainitic-austenitic microstructures, but additional quantitative phase analysis and high-resolution microstructural characterisation are required before the process can be described as an optimised route for producing nanobainite.

From an application-oriented point of view, the obtained results are important for designing heat treatments of medium-Mn multiphase steels intended for advanced high-strength steel applications [1,2,8]. In such alloys, the final properties are controlled not only by the chemical composition, but also by the phase balance obtained after processing [3,4,6]. Ferrite contributes to ductility and can improve formability, whereas bainitic or refined bainite-containing regions increase strength through microstructural refinement [6,26]. Retained austenite is particularly important because, if sufficiently stable, it can improve the strain-hardening capacity and delay strain localisation through the TRIP effect during deformation [3-5,9]. In contrast, fresh martensite formed during final cooling may increase hardness and strength locally, but its excessive fraction can reduce ductility and impair mechanical stability [3,5]. Therefore, the most promising heat-treatment conditions are those that combine a sufficient amount of transformable austenite, measurable bainitic transformation during IH, and thermal stability of the remaining austenite during final cooling [8,10,13,16,20]. In the present study, this combination was most clearly observed for the IA860/IH300 and IA870/IH300 samples.

5. Conclusions

The effect of intercritical annealing and isothermal holding conditions on the martensite start temperature, bainitic transformation response and retained austenite stability in 0.17C-3.1Mn-1.6Al-0.2Si-0.2Mo-0.04Nb multiphase steel was analysed using dilatometric measurements, thermodynamic calculations and SEM observations. The main findings of the study are:

1. The formation of refined bainite embedded in the intercritical austenite laths is only possible for properly selected isothermal holding conditions combining a moderate enrichment of intercritical austenite in C and Mn and corresponding austenite stability and moderate C diffusion rate in the bainitic transformation range close to the lowered M_s temperature.
2. Intercritical annealing temperature strongly affected the martensite start temperature of the investigated 0.17C-3.1Mn-1.6Al-0.2Si-0.2Mo-0.04Nb steel. Increasing IA temperature from 780 to 870°C increased M_s from approximately 170 to 305°C.
3. The decrease in M_s after lower-temperature IA is attributed to stronger C and Mn enrichment of intercritical austenite. However, lower IA temperatures also reduce the amount of austenite available for subsequent bainitic transformation.
4. The dilatometric response during isothermal holding depended on both IA and IH temperatures. Higher IA temperatures increased the amount of transformable austenite of moderate thermodynamic stability, whereas higher IH temperatures accelerated the transformation response within the investigated holding time.
5. Austenite remaining after IH was thermally stable during final cooling (RA islands) for most investigated variants. Martensitic transformation during final cooling was detected for the IA780/IH200 and IA800/IH220 samples, indicating insufficient stabilization of part of the remaining austenite under these conditions.
6. SEM observations revealed low-temperature bainite regions with refined morphology after the two-step heat treatments. However, further high-resolution characterization techniques are required in future studies to confirm the nanometric scale and quantify phase fractions.
7. Within the investigated range, the most favourable response among the tested heat-treatment conditions was observed for the IA860/IH300 and IA870/IH300 samples. These conditions combined a relatively large amount of transformable austenite with an IH temperature that enabled a measurable refined bainitic transformation response and did not produce a clear martensitic transformation signal during final cooling. The process should therefore be treated as a promising route for further optimization.

Funding

This research was funded in part by National Science Centre, Poland, through the grant no. 2021/41/N/ST8/03371. Mohammed Elmeligy acknowledges the financial support through the statutory funds of the Silesian University of Technology (Faculty of Mechanical Engineering), BKM2026 project.

REFERENCES

[1] J. Noder, J.E.T. Gutierrez, A. Zhumagulov, J. Dykeman, H. Ezzat, C.J. Butcher, A Comparative Evaluation of Third-Generation Advanced High-Strength Steels for Automotive Forming and Crash Applications. Materials **14** (17), 4970 (2021). DOI: https://doi.org/10.3390/ma14174970

[2] W. Bleck, F. Brühl, Y. Ma, C. Sasse, Materials and Processes for the Third-Generation Advanced High-Strength Steels. BHM Berg- Huettenmaenn. Monatsh. **164**, 466-474 (2019). DOI: https://doi.org/10.1007/s00501-019-00904-y

[3] A. Grajcar, A. Skowronek, R. Radwański, Mechanical Behavior and Stability of Dispersed Retained Austenite in Thermomechanically Rolled and Isothermally-Treated TRIP-Aided Multiphase Steel. Mater. Sci. Eng. A **831**, 142300 (2022). DOI: https://doi.org/10.1016/j.msea.2021.142300

[4] E.S. Perdahcioglu, H.J.M. Geijselaers, Mechanical Behavior of Multi-Phase Steels Comprising Retained Austenite. Materials **15** (2), 498 (2022). DOI: https://doi.org/10.3390/ma15020498

[5] P.J. Jacques, F. Delannay, J. Ladriere, On the Influence of Interactions Between Phases on the Mechanical Stability of Retained Austenite in Transformation-Induced Plasticity Multiphase Steels. Metall. Mater. Trans. A **32**, 2759-2768 (2001). DOI: https://doi.org/10.1007/s11661-001-1027-4

[6] A. Grajcar, W. Kwaśny, W. Zalecki, Microstructure-Property Relationships in TRIP Aided Medium-C Bainitic Steel with Lamellar Retained Austenite. Mater. Sci. Technol. **31** (7), 781-794 (2015). DOI: https://doi.org/10.1179/1743284714Y.0000000742

[7] A. Grajcar, K. Radwański, Microstructural Comparison of the Thermomechanically Treated and Cold Deformed Nb-Microalloyed TRIP Steel. Mater. Tehnol. **48** (5), 679-683 (2014). https://www.dlib.si/details/URN:NBN:SI:doc-ITYUMYLG?&-language=eng

[8] A. Grajcar, W. Zalecki, W. Burian, A. Kozlowska, Phase Equilibrium and Austenite Decomposition in Advanced High-Strength Medium-Mn Bainitic Steels. Metals **6** (10), 248 (2016). DOI: https://doi.org/10.3390/met6100248

[9] H. Xiao, G. Zhao, D. Xu, Y. Cheng, S. Bao, Effect of Microstructure Morphology of Q&P Steel on Carbon and Manganese Partitioning and Stability of Retained Austenite. Metals **12** (10), 1613 (2022). DOI: https://doi.org/10.3390/met12101613

[10] N. Yan, H. Di, R.D.K. Misra, H. Huang, Y. Li, Enhancing Austenite Stability in a New Medium-Mn Steel by Combining Deep Cryogenic Treatment and Intercritical Annealing: An Experimental and Theoretical Study. Mater. Sci. Eng. A **753**, 11-21 (2019). DOI: https://doi.org/10.1016/j.msea.2019.01.026

[11] A. Kokosza, J. Pacyna, Formation of Medium Carbon TRIP Steel Microstructure During Annealing in the Intercritical Temperature Range. Arch. Metall. Mater. **59** (3), 1017-1022 (2014). DOI: https://doi.org/10.2478/amm-2014-0170

[12] Z.H. Cai, H.Y. Li, S.Y. Jing, Z.C. Li, H. Ding, Z.Y. Tang, R.D.K. Misra, Influence of Annealing Temperature on Microstructure and Tensile Property of Cold-Rolled Fe-0.2C-11Mn-6Al Steel. Mater. Charact. **137**, 256-262 (2018). DOI: https://doi.org/10.1016/j.matchar.2018.01.043

[13] B. Hu, H. Luo, A Novel Two-Step Intercritical Annealing Process to Improve Mechanical Properties of Medium Mn Steel. Acta Mater. **176**, 250-263 (2019). DOI: https://doi.org/10.1016/j.actamat.2019.07.014

[14] G.J. Lin, H. Lan, L. Du, Modelling and Experimental Validation of Austenite Growth from As-Quenched Martensite During Intercritical Annealing of a Medium-Mn Steel. J. Mater. Sci. **56** (34), 19165-19179 (2021). DOI: https://doi.org/10.1007/s10853-021-06482-0

[15] G. Liu, L. Ba, S. Xu, S. Tong, X. Wang, X. Liang, X. Sun, Effect of Intercritical Annealing Temperature on Multiphase Microstructure Evolution in Ultra-Low Carbon Medium Manganese Steel. Mater. Charact. **173**, 110920 (2021). DOI: https://doi.org/10.1016/j.matchar.2021.110920

[16] A. Skowronek, A. Grajcar, A. Kozłowska, A. Janik, M. Morawiec, R.H. Petrov, Temperature-Dependent Microstructural Evolution of Al-Rich Medium-Mn Steel During Intercritical Annealing. Metall. Mater. Trans. A **53** (8), 3012-3021 (2022). DOI: https://doi.org/10.1007/s11661-022-06721-2

[17] M. Morawiec, A. Grajcar, W. Zalecki, C. Garcia-Mateo, M. Opiela, Dilatometric Study of Phase Transformations in 5Mn Steel Subjected to Different Heat Treatments. Materials **13** (4), 958 (2020). DOI: https://doi.org/10.3390/ma13040958

[18] A. Skowronek, A. Kozłowska, Thermodynamic-Kinetic Calculations and Dilatometric Verification of the Martensitic and Bainitic Transformations in 4% Medium-Mn Steel. J. Therm. Anal. Calorim. **150**, 1069-1079 (2025). DOI: https://doi.org/10.1007/s10973-024-13662-y

[19] A. Skowronek, A. Kozłowska, Phase Transitions in Medium-Mn Alloy: Thermodynamic Simulation and Experimental Verification. J. Therm. Anal. Calorim. **150**, 1059-1068 (2025). DOI: https://doi.org/10.1007/s10973-024-13824-y

[20] M. Morawiec, J. Opara, C. Garcia-Mateo, J.A. Jimenez, A. Grajcar, Effect of Mn on the Chemical Driving Force and Bainite Transformation Kinetics in Medium-Manganese Alloys. J. Therm. Anal. Calorim. **148**, 1567-1576 (2023). DOI: https://doi.org/10.1007/s10973-022-11664-2

[21] J.H. Kim, G. Gu, S.H. Hong, C.J. Yu, M. Koo, E.Y. Kim, A. Zargaran, J.S. Lee, D.W. Suh, Acceleration of Bainitic Transformation in 0.28C-3.8Mn-1.5Si Steel Utilizing Chemical Heterogeneity. Scr. Mater. **239**, 115779 (2024). DOI: https://doi.org/10.1016/j.scriptamat.2023.115779

[22] M. Morawiec, J. Opara, A. Skowronek, A. Kalhor, A. Kozłowska, A. Wojtacha, A. Grajcar, Influence of Mn on Nanobainite Formation Kinetics and Austenite Retention in Al-Added Medium-Mn Steels Subjected to Hybrid Isothermal Annealing. J. Mater. Res. Technol. **37**, 549-562 (2025). DOI: https://doi.org/10.1016/j.jmrt.2025.05.256

[23] A. Wojtacha, A. Kozłowska, A. Skowronek, O. Gülbay, J. Opara, A. Gramlich, K. Matus, Design Concept and Phase Transformation Study of Advanced Bainitic-Austenitic Medium-Mn Steel. Sci. Rep. **15**, 22843 (2025). DOI: https://doi.org/10.1038/s41598-025-05854-9

[24] J. Zhu, X. Sun, G. Barber, X. Han, H. Qin, Effect of Carbon Content on Bainite Transformation Kinetics and Microstructure of 4140/4150 Steels. Eur. Sci. J. **15** (9), 518-536 (2019). DOI: https://doi.org/10.19044/esj.2019.v15n9p518

[25] W. Pei, W. Liu, Y. Zhang, R. Qie, A. Zhao, Study on Kinetics of Transformation in Medium Carbon Steel Bainite at Different Isothermal Temperatures. Materials **14** (11), 2721 (2021). DOI: https://doi.org/10.3390/ma14112721

[26] A. Skowronek, E. Cordova-Tapia, P. Tobajas-Balsera, C. Garcia-Mateo, J.A. Jimenez, R. Petrov, A. Grajcar, Bainite Plate Thickness Reduction and Microstructure Tailoring by Double Austempering of Al-Rich 3Mn Steel. Mater. Sci. Eng. A **853**, 143743 (2022). DOI: https://doi.org/10.1016/j.msea.2022.143743

[27] S. Kaar, D. Krizan, R. Schneider, C. Sommitsch, Impact of Si and Al on Microstructural Evolution and Mechanical Properties of Lean Medium Manganese Quenching and Partitioning Steels. Steel Res. Int. **91** (10), 2000181 (2020). DOI: https://doi.org/10.1002/srin.202000181

[28] M.S. Węglowski, J. Marcisz, B. Garbarz, Technological Properties and Applications of High-Carbon Nanobainitic Steels. Biul. Inst. Spaw. **3**, 29-43 (2018). DOI: https://doi.org/10.17729/ebis.2018.3/3

[29] L. Morales-Rivas, Viewpoints on Technological Aspects of Advanced High-Strength Bainitic Steels. Metals 12 (2), 195 (2022). DOI: https://doi.org/10.3390/met12020195

[30] O. Ríos-Diez, R. Aristizábal-Sierra, C. Serna-Giraldo, J.A. Jimenez, C. Garcia-Mateo, Development of Nanobainitic Microstructures in Carbo-Austempered Cast Steels: Heat Treatment, Microstructure and Properties. Metals **10** (5), 635 (2020). DOI: https://doi.org/10.3390/met10050635

[31] ASTM A1033-04, Standard Practice for Quantitative Measurement and Reporting of Hypoeutectoid Carbon and Low-Alloy Steel Phase Transformations, ASTM International, West Conshohocken (2004). https://www.astm.org/, accessed: 2026-04-29

[32] Sente Software Ltd., A Collection of Free Downloadable Papers on the Development and Application of JMatPro (2005). https://www.sentesoftware.co.uk/biblio.html, accessed: 2026-04-29

[33] J.O. Andersson, T. Helander, L. Höglund, P. Shi, B. Sundman, Thermo-Calc & DICTRA, computational tools for materials science. Calphad **26**, 273-312 (2002). DOI: https://doi.org/10.1016/S0364-5916%2802%2900037-8

[34] M. Peet, H.K.D.H. Bhadeshia, MAP_STEEL_MUCG83, Materials Algorithms Project (MAP), Department of Materials Science and Metallurgy, University of Cambridge, U.K. https://www.phase-trans.msm.cam.ac.uk/map/steel/programs/mucg83.html, accessed: 2026-04-29